

# Water vapour column abundance retrieval using multispectral radiometer measurements in Sydney, Australia

Ghassan Taha\* and Gail P. Box

School of Physics, University of New South Wales, Sydney, Australia.

(Manuscript received February 2001; revised June 2002)

**Water vapour column abundances in Sydney were derived from Multifilter Rotating Shadowband Radiometer (MFRSR) solar transmittance measurements in the 0.934  $\mu\text{m}$  band using the modified Langley technique. The atmospheric models LOWTRAN 7 and MODTRAN 3 were used to calculate the water vapour transmittance in the region centred at 0.934  $\mu\text{m}$ , in order to determine the instrument coefficients required for water vapour retrieval. We also propose the use of eigenvalue analysis to predict aerosol optical thickness at the water vapour channel, in comparison to the quadratic form relationship.**

**Long-term measurements were used to study the diurnal and temporal variability of water vapour column abundances. An apparent seasonal pattern of maximum water vapour column values during the summer season and minimum values during the winter season was observed during a whole year of measurements.**

## Introduction

Water vapour plays a crucial role in atmospheric processes, from global climate to micrometeorology. It is the most variable major constituent of the atmosphere and the largest contributor to the greenhouse effect. It affects the global climate system directly, by absorbing and radiating energy from the sun, and indirectly, by its effect on cloud formation, aerosol growth, and the chemistry of the lower atmosphere. It plays a critical role in many of the chemical reactions that occur in the atmosphere.

For many years, radiosondes were the main means of measuring the water vapour column throughout the atmosphere, however they are labour intensive and, because of the high costs, are only launched twice a day thus seriously under-sampling temporal variability. Sun photometers or radiometers, which are usually used for aerosol measurements, offer an alternative to radiosondes for retrieving column abundances of water vapour, when an appropriate filter is used, such as the 0.940  $\mu\text{m}$  band. They are easily operated and provide continuous measurements during the day-time, with a minimum cost. The disadvantages of these instruments are that they can provide data only under clear sky conditions, and they do not recover vertical profile information. In recent times, radiometers increasingly have been used to measure atmos-

---

*Corresponding author address:* Gail Box, School of Physics, University of New South Wales, Sydney, NSW 2052, Australia.  
Email: gpb@newt.phys.unsw.edu.au

\*Now at University of Arizona and NASA Langley Research Center, Hampton, Virginia.

pheric transmission in the visible and near IR. Several studies have been made estimating the column water vapour amount using the absorption in the  $\lambda = 0.940 \mu\text{m}$  region (e.g. Bruegge et al. 1992; Thome et al. 1992, 1993; Frouin et al. 1990; Michalsky et al. 1995; Shiobara et al. 1996).

The next section outlines the methods used in this study. We discuss the water vapour column abundance retrieval from the Multifilter Rotating Shadowband Radiometer (MFRSR) (Harrison et al. 1994) for solar transmittance measurements in the 0.934 mm band, using the modified Langley technique of Bruegge et al. (1992). A new method for retrieving aerosol optical thickness at  $\lambda = 0.934 \mu\text{m}$  using eigenvalue analysis is proposed, and compared with aerosol optical thickness predicted using the quadratic form proposed by King and Byrne (1976). The use of the atmospheric transmission models LOWTRAN 7 and MODTRAN 3 for determining the instrument coefficients required for water vapour retrieval is also investigated.

Results of the inferred temporal and seasonal variations of the water vapour column abundance in Sydney are presented and analysed, along with a comparison between a subset of the radiometer data and corresponding radiosonde data. The final section provides a summary of the results, conclusions and recommendations for further work.

## Methodology

Aerosol spectral optical thickness was measured on a daily basis using an MFRSR located on the Kensington campus of the University of New South Wales, in Sydney's eastern suburbs, at  $33^\circ 55' 11.6'' \text{S}$  and  $151^\circ 13' 40.7'' \text{E}$ , and 85 m above sea level. It has one broad band, and six narrow bands ( $\lambda = 0.4154, 0.5017, 0.6155, 0.6727, 0.8698$  and  $0.9336 \mu\text{m}$ ), of which the first five are used to extract aerosol optical thickness data. On all suitable days, a Langley analysis was performed on both the morning and afternoon data to obtain the atmospheric optical depth at each of these wavelengths.

### Modified Langley plot

In order to compute the water vapour transmittance, it is necessary to first remove the influence of molecular and aerosol scattering. In narrow band filters, which are usually used in radiometers to measure the direct solar irradiance under clear sky conditions, spectral attenuation of light is described by

$$V_\lambda = V_{o\lambda} R^{-2} \exp(-\tau_\lambda m) \quad \dots 1$$

or

$$\ln(V_\lambda) = \ln(V_{o\lambda} R^{-2}) - \tau_\lambda m \quad \dots 2$$

where  $V_\lambda$  is the instrument output voltage,  $V_{o\lambda}$  is the instrument calibration constant,  $R$  is the Earth-Sun distance in astronomical units,  $\tau_\lambda$  is the optical thickness and the airmass,  $m$ , is the secant of the solar zenith angle,  $\theta$ . However, in regions of strong spectral variation of molecular absorption, the relationship must be modified to include water vapour effects:

$$V_\lambda = V_{o\lambda} R^{-2} \exp(-\tau_\lambda m) T_w \quad \dots 3$$

where  $T_w$  is the water vapour transmittance. Since gaseous absorption is not linear in air mass, it cannot be resolved using the standard Langley method. Bruegge et al. (1992) used a modified Langley approach. For measurements of the  $0.934 \mu\text{m}$  channel, the argument of the exponential term in Eqn 2 is modified so that

$$\tau_\lambda m \rightarrow (\tau_R + \tau_{aer}) [u]^n + k(um)^b$$

where  $\tau_R$  and  $\tau_{aer}$  are the Rayleigh and aerosol optical thickness components respectively,  $u$  is the column water vapour, and  $k$  and  $b$  are constants of a particular filter. The modified equation is then displayed in logarithmic form as

$$\ln(V) + (\tau_R + \tau_{aer}) m = \ln(V_o R^{-2}) - k(um)^b \quad \dots 4$$

with the subscripts  $\lambda$  omitted for simplicity.

A plot of  $\ln(V) + (\tau_R + \tau_{aer}) m$  against  $m^b$  for clear and stable days, with assumed homogenous water vapour distribution, will yield a straight line with a slope  $ku^b$  and a y-intercept of  $\ln(V_o R^{-2})$ . Usually intervals in the morning and the afternoon, when  $m$  lies between 2 and 6, are used. In order to solve this equation for  $u$ , we need to determine  $k$  and  $b$  from transmittance modelling, and  $\tau_{aer}$  from measurements.

### Prediction of aerosol optical thickness

In order to apply the modified Langley technique, aerosol optical thickness,  $\tau_{aer}$ , needs to be known. At  $\lambda = 0.934 \mu\text{m}$ ,  $\tau_{aer}$  may be predicted from other optical thickness measurements, after corrections for Rayleigh scattering and ozone absorption are made, using both the eigenvalue analysis technique, and the quadratic form. Eigenvalue analysis has been successfully used to separate the aerosol and ozone contributions for the  $\lambda = 0.502, 0.615$  and  $0.673 \mu\text{m}$  channels with one to two per cent accuracy (Taha and Box 1999). Here we are proposing the use of the same technique to predict the aerosol contribution at  $\lambda = 0.934 \mu\text{m}$ .

The eigenvalue analysis technique is based on the fact that aerosol optical thickness,  $\tau_{aer}(\lambda)$ , is related to the size distribution by

$$\tau_{aer}(\lambda) = \int \pi r^2 Q(r, \lambda, m) n(r) dr \quad \dots 5$$

where  $Q$  is the Mie extinction efficiency,  $m$  is the complex refractive index,  $r$  is the particle radius and  $n(r)$  is the number of particles per unit area per unit radius in a vertical column through the atmosphere with radii between  $r$  and  $r + dr$ . Twomey (1974, 1977) has shown that, because the kernels of this equation are not independent of one another, one kernel (or measurement) can be predicted as a linear combination of the others within the measurement error. The coefficients for this linear combination are derived from the eigenvectors of the kernel covariance matrix (Box et al. 1996; Taha and Box 1999).

After correcting for ozone absorption using eigenvalue analysis, the aerosol contribution at 0.934  $\mu\text{m}$ ,  $\tau_m$ , was calculated from the measurements at the other wavelengths,  $\tau_i$ , using

$$\tau_m = \sum_{j \neq m} b_j \tau_i \quad \dots 6$$

The coefficients,  $b_j$ , were calculated for three different types of aerosol, using the eigenvector associated with the smallest eigenvalue. Values of these coefficients are given in Table 1.

King and Byrne (1976) proposed a method, referred to here as the quadratic form, to predict the total ozone column, assuming a quadratic dependence between the natural logarithm of the aerosol optical thickness, and the natural logarithm of the wavelength. After corrections for ozone absorption were made using this method, the same quadrature form, Eqn 7, was used to extrapolate for  $\tau_{aer}$  at 0.934  $\mu\text{m}$ , as proposed by Michalsky et al. (1995), namely

$$\ln(\tau_{aer}) = a + b \ln(\lambda) + c[\ln(\lambda)]^2 \quad \dots 7$$

Both of these methods are used in the results section.

### Water vapour transmittance modelling

To convert measured water vapour transmittance,  $T_w$ , into  $u$ , theoretical models are used to determine  $T_w$ , centred at a particular filter wavelength,  $\lambda$ , along a slant path of  $m$  by

$$T_w(\lambda) = \frac{\int_{\Delta\lambda} T(\lambda) f(\lambda) d\lambda}{\int_{\Delta\lambda} f(\lambda) d\lambda} \quad \dots 8$$

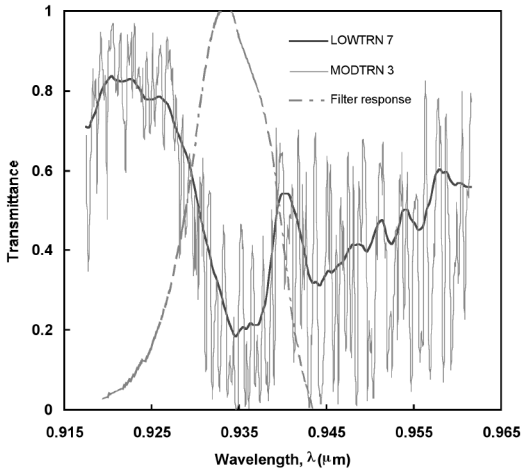
$T_w$  is the transmittance due to the gas absorption, calculated with respect to the equivalent total absorber amount, which is accumulated along the slant path  $m$ , and  $f(\lambda)$  is the filter function or spectral response. The relative response for the MFRSR water vapour filter was measured by the manufacturer at 24 different wavelengths using a monochromator. To perform more accurate integration of the above equation, 275 more wavelengths were obtained by interpolating between measurement points using a polynomial fit to selected parts of the curve.  $T_w$  is usually calculated using atmospheric transmittance models. In this work we have used LOWTRAN 7 (Kneizys et al. 1988) and MODTRAN 3 (Berk et al. 1989; Anderson et al. 1993). The main difference between the two models is the spectral resolution: 20  $\text{cm}^{-1}$  and 2  $\text{cm}^{-1}$  respectively. Figure 1 is a plot of the transmittance modelled using LOWTRAN 7 and MODTRAN 3 along a vertical path through the midlatitude summer atmosphere, with a 2.92 cm vertical column of water vapour, and the spectral response for the MFRSR channel.

LOWTRAN 7 and MODTRAN 3 calculations were performed in the transmittance mode with no aerosol loading and midlatitude summer conditions. Water vapour transmittance was calculated from sea level to the top of atmosphere, in the spectral region  $\lambda = 0.920$  to 0.960  $\mu\text{m}$ , for solar zenith angles,  $\theta_s = 0^\circ$  to  $85^\circ$ , which corresponds to  $m \approx 1$  to 11. Other studies showed differences of less than one per cent between midlatitude summer, winter and tropical model atmospheres (Michalsky et al. 1995; Halthore et al. 1997). Therefore there was no need to repeat

**Table 1. Coefficients used for prediction of 0.934  $\mu\text{m}$  measurement for MFRSR wavelengths.**

Aerosol Type	Wavelength, $\lambda$ ( $\mu\text{m}$ )				
	0.414	0.502	0.616	0.673	0.870
Average Continental	-0.001	-0.018	0.415	-0.709	1.301
Urban	-0.047	0.093	0.423	-0.865	1.391
Dust-like	0.009	-0.056	0.459	-0.709	1.282

**Fig. 1** The MFRSR narrow-band filter transmittance superimposed on atmospheric water vapour transmittance for midlatitude summer with a water content of 2.92 cm of precipitable water, as computed by LOWTRAN 7 and MODTRAN 3.



this calculation for other conditions.

The next step was to calculate the wavelength integrated transmittance,  $T_w$ , using Eqn 8. Results of the calculation may be expressed in a two-parameter model as

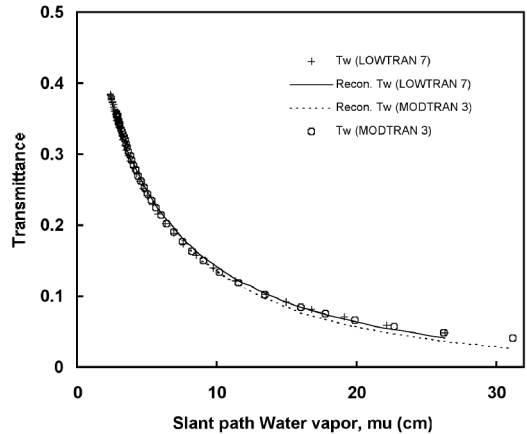
$$T_w = \exp[-k(um)^b] \quad \dots 9$$

Figure 2 is the water vapour integrated transmittance,  $T_w$ , plotted versus slant path water vapour amount, in cm, determined using LOWTRAN 7 and MODTRAN 3. In order to obtain coefficients  $k$  and  $b$ , Eqn. 9 needs to be rearranged into logarithmic form as

$$\ln(\ln(1/T_w)) = \ln(k) + b \ln(um) \quad \dots 10$$

A plot of  $\ln(\ln(1/T_w))$  versus  $\ln(um)$  should give a straight line with slope  $b$ , and  $y$ -intercept  $\ln(k)$ . Figure 3 is a plot of  $\ln(\ln(1/T_w))$  versus  $\ln(um)$ , determined by LOWTRAN 7 and MODTRAN 3. Both curves show a regression fit  $R^2$  very close to 1.0. Table 2 is a summary of the coefficients  $k$  and  $b$  obtained, and the reconstructed  $T_w$  is also shown in Fig. 2. It is obvious that there is a small difference between the values of the coefficients obtained by LOWTRAN 7 and MODTRAN 3, which is caused mainly by the different spectral resolution of the models. We believe that the values obtained by MODTRAN 3 are more accurate,

**Fig. 2** Water vapour integrated transmittance  $T_w$ , determined using LOWTRAN 7 (plus) and MODTRAN 3 (circle), versus slant path water vapour amount. The reconstructed  $T_w$  was determined using  $k = 0.5739$ ,  $b = 0.4862$  (LOWTRAN 7, solid curve) and  $k = 0.6053$ ,  $b = 0.5184$  (MODTRAN 3, dotted curve).



and we chose to use only these coefficients.

Schmid et al. (1996) compared modelled and empirical approaches for retrieving column water vapour from solar transmittance measurements in the 0.940  $\mu\text{m}$  region. They found that, with respect to experimental data, LOWTRAN 7 and MODTRAN 3 resulted in an overestimation in  $T_w$  retrieval of 18-30 per cent and 7-20 per cent respectively. Michalsky et al. (1995) used MODTRAN 2 for their water vapour column retrieval from MFRSR data and comparison between a microwave radiometer and the MFRSR resulted in a root-mean-square difference of 12 per cent compared to the mean value, with the MFRSR having a small positive bias relative to the microwave radiometer.

## Results

**Table 2.** Coefficients  $k$  and  $b$  obtained for the MFRSR using LOWTRAN 7 and MODTRAN 3, mid-latitude summer,  $R^2$  is the regression coefficient for the line of best fit.

Model	$k$	$b$	$R^2$
LOWTRAN 7	0.5739	0.4862	0.998
MODTRAN 3	0.6053	0.5184	0.9993

**Fig. 3** A plot of  $\ln(\ln(1/T_w))$ , determined using LOWTRAN 7 (cross) and MODTRAN 3 (circle), versus  $\ln(\mu m)$ . The slope of the line is  $b$ , while  $k$  is the log of the y-intercept.

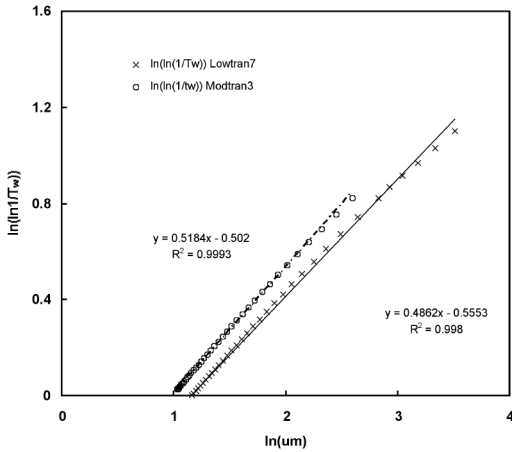
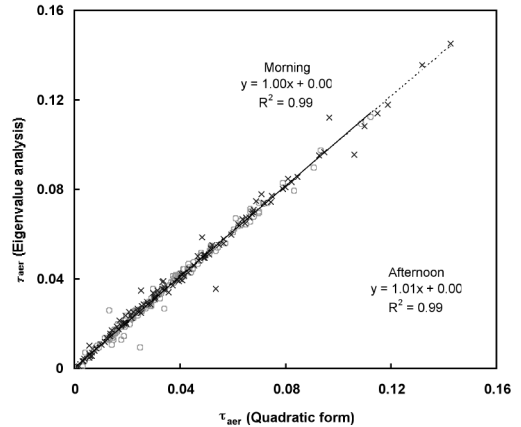
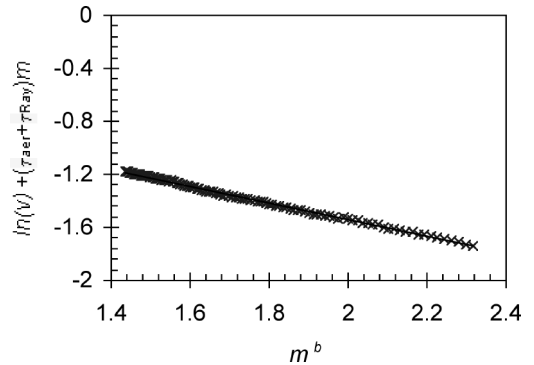


**Fig. 4** Predicted aerosol optical thickness,  $\tau_{aer}$ , at  $\lambda = 0.934 \mu m$  for both the morning (cross) and afternoon (circle), using eigenvalue analysis versus  $\tau_{aer}$  predicted by quadratic form.



Both the eigenvalue analysis and the quadratic relationship were used to predict the aerosol optical thickness,  $\tau_{aer}$  at  $\lambda = 0.934 \mu m$ , using the measurements of an MFRSR for 155 days, with a clear period in either or both the morning and afternoon. The coefficients given in Table 1 for average continental aerosol were used to predict the aerosol component of the  $0.934 \mu m$  channel. Figure 4 is a plot of the predicted  $\tau_{aer}$  using eigenvalue analysis, versus  $\tau_{aer}$  using the quadratic form, for the morning and afternoon data. Both curves showed a slope  $\approx 1$ , and a y-intercept  $\approx 0.0$ , with a regression coefficient of  $R^2 = 0.99$ . The values of  $\tau_{aer}$  predicted by the two methods differed by less than one per cent and thus, because of the minimal effect of the aerosol optical thickness compared to the water vapour contribution in the  $0.934 \mu m$  channel, either method can be used for the aerosol correction.

**Fig. 5** Modified Langley plot for the morning of 29 April 1997.  $\tau_{aer} = 0.0422$ ,  $\tau_R = 0.012$ . Solid line is the least square best fit line.



**Column water vapour retrieval**

The continuous water vapour column can be estimated by combining Eqns 3 and 9

$$u = \frac{1}{m} \left[ \frac{1}{k} \left( \ln \left( \frac{V_o R^2}{V} \right) - m(\tau_{aer} + \tau_R) \right) \right]^{\frac{1}{b}} \dots 11$$

In order to solve this equation, it is necessary to know the value of the MFRSR channel calibration constant  $V_o$ . This was found using the modified Langley technique as described above. Figure 5 is a Langley plot

and the least squares best fit line for the morning of 29 April 1997, which was a fairly clear and stable day. Accurate determination of  $V_o$  requires that the water vapour in the atmosphere be stable over the measurement period and this was generally not the case. Since  $V_o$  should not vary from day to day, an average value

**Fig. 6** Water vapour column retrieval,  $u$  ( $\text{gm cm}^{-2}$ ), on 10 June 1997. Local time is UTC + 10h.

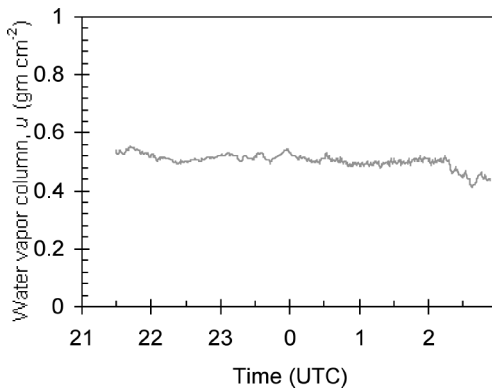
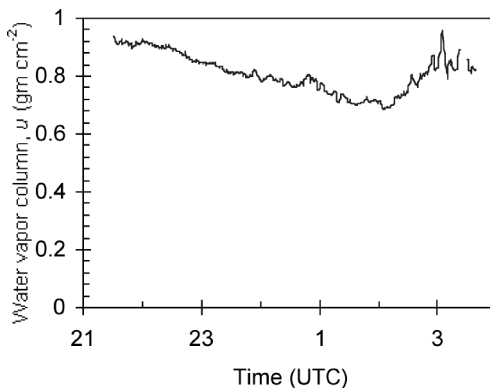


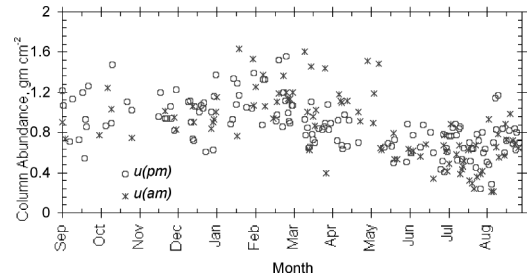
**Fig. 7** Water vapour column retrieval,  $u$  ( $\text{gm cm}^{-2}$ ), on 29 April 1997. Local time is UTC + 10h.



of  $V_o$  was determined for the entire set of measurements. The estimated  $V_o$  did not show any apparent trend with time. The computed average value of the calibration constant was  $V_o = 0.689 V$  with a standard deviation  $\sigma = 0.083 V$ . This error reflects errors due to the nature of the analysis rather than day-to-day fluctuations. Errors introduced by an error in  $V_o$  are complex and depend on both the air mass and the amount of water vapour, ranging from up to 40 per cent for  $m = 2$  and  $u = 0.5 \text{ g cm}^{-2}$  to 13 per cent for  $m = 6$  and  $u = 2 \text{ g cm}^{-2}$ . If the value of  $V_o$  used is too low, the value of  $u$  will be underestimated.

Figures 6 and 7 show temporal variation of the water vapour column,  $u$  ( $\text{gm cm}^{-2}$ ), as observed by the

**Fig. 8** Temporal variation of the averaged water vapour column,  $u$  ( $\text{gm cm}^{-2}$ ), as observed by the MFRSR From 25 September 1996, to 16 September 1997, for the morning (cross) and afternoon (circle) periods.



MFRSR 0.934  $\mu\text{m}$  channel, for 10 June and 29 April 1997 respectively. Variability of the water vapour column with time was relatively small during 10 June, with a fairly low value of  $u \approx 0.5 \text{ gm cm}^{-2}$ . On the other hand, it was reasonably unstable during 29 April, with a higher average water vapour column of  $u \approx 0.9 \text{ gm cm}^{-2}$ .

Figure 8 is a plot of the averaged water vapour column retrieval,  $u$  ( $\text{gm cm}^{-2}$ ), derived using the Modified Langley technique, for the morning and afternoon periods, measured from 25 September 1996 to 16 September 1997. It shows an apparent seasonal variation, where the maximum observed values of  $u$  were measured during the summer season (December, January, and February), while the smallest values of  $u$  were measured during the winter season (June, July, and August). A similar seasonal pattern was observed by Halthore et al. (1997), who presented results of the amount of precipitable water derived from a narrow-band Cimel sun photometer network around the world. Water vapour retrieval showed a similar seasonal variation with high values during summer, and low values during winter.

### Comparison with radiosonde measurements

In order to validate the radiometer water vapour column retrievals we obtained radiosonde profile data for Sydney Airport from the Bureau of Meteorology. This data included pressure,  $P$ , geopotential height,  $Z$ , dew-point temperature,  $T_d$ , and air temperature,  $T_{air}$ . Using this information the mixing ratio,  $r$  in  $\text{g/kg}$ , was calculated at each pressure level. Using the Clausius - Clapeyron equation for the partial pressure of water vapour,  $e$ , we have:

$$r = \varepsilon \frac{e}{P} = \frac{6.11 \times 622}{P} \exp\left[\frac{L}{R_v} \left(\frac{1}{273} - \frac{1}{T_d}\right)\right] \dots 12$$

where pressures are in hectopascals,  $\varepsilon = 0.622$  is the ratio of the molecular weight of moist air to the molecular weight of dry air,  $L = 2500 \text{ kJ kg}^{-1}$  is the latent heat of vapourisation, and  $R_v = 461.5 \text{ J kg}^{-1} \text{ K}^{-1}$  is the gas constant for water vapour. Air density at each pressure level was determined using the ideal gas equation and the mixing ratio was converted to  $\text{gm}^{-3}$  by multiplying by the air density at that level. The total precipitable water was then found by integrating the mixing ratio over geopotential height using a simple trapezoidal scheme. The radiosondes were launched at 2000 UTC and 0500 UTC (6 am and 3 pm local time).

Comparisons between radiosonde data and radiometer data for the months of February, April, June and August showed that the radiosonde values were generally higher than the radiometer values. This can be seen in Fig. 9 which is a scatter plot of the afternoon radiosonde water vapour values against those derived from the radiometer using both MODTRAN 3 and LOWTRAN 7. The parameters and statistics for the afternoon regression fits are given in Table 3. Although the radiosonde and radiometer values are clearly correlated, there is a large degree of scatter. It should be noted that the radiometer values used in the scatter plot are effectively averages over the whole afternoon, which, given the variability of water vapour, may provide a partial explanation for the observed discrepancies. Similar results were obtained for the morning although the correlations were lower, which is to be expected, because the morning radiometer measurements generally do not overlap the morning radiosonde launches.

**Fig. 9** Radiosonde derived water vapour column versus radiometer derived water vapour column for afternoon, February 1997, April 1997, June 1997 and August 1997.

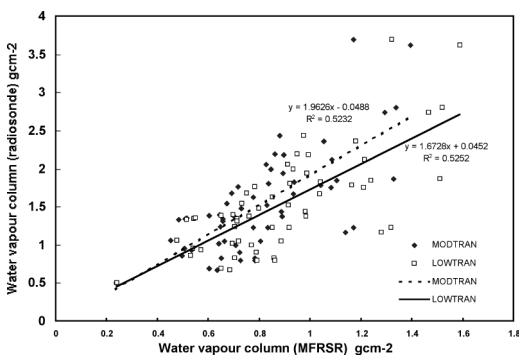


**Table 3.** Parameters and statistics for regression of afternoon radiosonde vs afternoon radiometer measurements using both LOWTRAN 7 and MODTRAN 3.

Model	Slope	Intercept	R <sup>2</sup>
LOWTRAN 7	1.673 ± 0.217	0.045 ± 0.203	0.525
MODTRAN 3	1.963 ± 0.255	-0.049 ± 0.215	0.523

Comparison between radiosonde values and the continuous trace values also showed that the radiometer values were often lower than the radiosonde values. It was difficult to draw firm conclusions about this because the radiometer trace did not always overlap the radiosonde launch times, and the number of days for which the continuous trace is available is small.

Comparison of radiosonde data and radiometer data is complicated by a number of other factors, which are outlined below. Sydney Airport is several kilometres from the University and, because it is on the coast, it is likely that there will be differences in the water vapour profile at the two locations, with higher water content most likely at the airport. In addition, the radiosonde profiles start at 5 m whereas the radiometer is 85 m above sea level, and this would result in lower values from the radiometer. No attempt was made to correct for these factors because any assumptions made in doing so would introduce additional errors which would be difficult to quantify. The use of co-located instruments would reduce this type of error.

Another likely source of discrepancy is the transmittance modelling, since the accuracy of the modelling depends on how well the water vapour is parameterised in the model. It is beyond the scope of this paper to investigate this potential source of error, however there are several ways of improving the transmittance modelling in future studies. Water vapour profiles derived from on-site data rather than standard models should result in better parametrisation and this is recommended for further studies. In this work two transmittance models have been used, other models should also be investigated to see if they are more appropriate.

It is clear that there is reasonable correlation between the radiometer and radiosonde derived values for the water vapour column, although there are a number of steps which should be taken to improve future work. What has been demonstrated here, however, is the potential of multispectral radiometer based retrieval methods for providing information about the temporal

behaviour of water vapour, even if it is largely qualitative. This will complement radiosonde measurements and, with co-located instruments and improved transmittance modelling, it should be possible to establish a stronger cross calibration between the two.

## Summary and conclusions

The Multifilter Rotating Shadowband Radiometer (MFRSR) solar transmittance measurements in the 0.934  $\mu\text{m}$  band were used to retrieve the water vapour column abundance, using the modified Langley technique. Atmospheric transmittance models LOWTRAN 7 and MODTRAN 3 were used to calculate the water vapour transmittance, centred at  $\lambda = 0.934\mu\text{m}$ , for different solar zenith angles, in order to obtain the instrument coefficients  $k$  and  $b$ .

An alternative method to predict the aerosol optical thickness at  $\lambda = 0.934 \mu\text{m}$ , using eigenvalue analysis was introduced and compared with the aerosol optical thickness predicted using the quadratic form relationship, proposed by King and Byrne (1976). Both methods produced similar results for aerosol optical thickness. The difference between the two predicted values was less than one per cent, and insignificant compared to the effect of water vapour transmittance. However, the eigenvalue analysis technique will provide a fast, reliable, and easy to use alternative for such predictions.

Temporal and seasonal variations of the water vapour column abundance were investigated. An apparent seasonal pattern of maximum water vapour column values during summer and minimum values during winter was observed during a whole year of measurements. Long-term measurements will help in building up a comprehensive database of the seasonal and inter annual variations of the water vapour column in Sydney, and lead to improvements in modelling efforts to determine its direct radiative impacts on climate.

In this paper we have outlined a technique using multispectral radiometers to retrieve column water vapour and also provide a continuous trace of its variation throughout the day. This technique has the potential to complement the twice daily radiosonde measurements. A number of steps which should lead to better correlation between the radiometer and radiosonde measurements in the future have been identified. The two most important are the use of a co-located radiometer and radiosonde to minimise differences resulting from spatial variability of the water vapour column, and a detailed analysis of the transmittance modelling. The transmittance modelling should be site specific, using a locally determined

water vapour profile, and other models besides those used here should be considered.

## References

- Anderson, G.P., Chetwynd, J.H., Theriault, J.-M., Acharaya, P., Berk, A., Robertson, D.C., Kneizys, F.X., Hooke, M.L., Abreu, L.W. and Shettle, E.P. 1993. MODTRAN 2: Suitability for remote sensing, In Proceeding of SPIE Int. Soc. Opt. Eng., *Atmospheric Propagation and Remote Sensing II*, 514-25.
- Berk, A., Bernstein, L.S. and Robertson, D.C. 1989. MODTRAN: A Moderate Resolution Model for LOWTRAN 7, GL-TR-89-0122, *Technical report*, Geophysics Dir., Phillips Lab., Hanscom Air Force Base, Mass.
- Box, G.P., Box, M.A. and Krücker, J. 1996. Information content and wavelength selection for multispectral radiometers. *J. geophys. Res.*, *101*, 19,211-14.
- Bruegge, C.J., Conel, J.E., Green, R.O., Margolis, J.S., Holm, R.G. and Toon, G. 1992. Water vapor column abundance retrievals during FIFE. *J. geophys. Res.*, *97*, 18,759-68.
- Frouin, R., Deschamps, P. and Lecomte, P. 1990. Determination from space of atmospheric total vapor amounts by differential absorption near 940 nm: Theory and airborne verification. *Jnl appl. Met.*, *29*, 448-59.
- Halothore, R.N., Eck, T.F., Holben, B.N. and Markham, B.L. 1997. Sun photometric measurements of atmospheric water vapor column abundance in the 940-nm band. *J. geophys. Res.*, *102*, 4343-52.
- Harrison, L., Michalsky, J. and Berndt, J. 1994. Automated Multifilter Rotating Shadow-Band Radiometer: An instrument for optical depth and radiation measurements. *Appl. Opt.*, *33*, 5118-25.
- King, M.D. and Byrne, D.M. 1976. A method for inferring total ozone content from the spectral variation of total optical depth obtained with a solar radiometer. *J. Atmos. Sci.*, *33*, 2242-51.
- Kneizys, F.X., Shettle, E.P., Abreu, L.W., Chetwynd, J.H., Anderson, G.P., Gallery, W.O., Selby, J.E.A. and Clough, S.A. 1988. *Users Guide to LOWTRAN 7*, AFGL-TR-88-0177, 137 pp.
- Michalsky, J.J., Liljegren, J.C. and Harrison, L.C. 1995. A comparison of sun photometer derivations of total column water vapor and ozone to standard measures of same at the Southern Great Plains Atmospheric Radiation Measurement site. *J. geophys. Res.*, *100*, 25,995-26,003.
- Schmid, B., Thome, K.J., Demoulin, P., Peter, R., Mätzler, C. and Sekler, J. 1996. Comparison of modeled and empirical approaches for retrieving columnar water vapor from solar transmittance measurements in the 0.94- $\mu\text{m}$  region. *J. geophys. Res.*, *101*, 9,345-58.
- Shiobara, M., Spinhirne, J.D., Uchiyama, A. and Asano, S. 1996. Optical depth measurements of aerosol clouds and water vapor using sun photometers during FIRE Cirrus IFO II. *Jnl appl. Met.*, *35*, 36-46.
- Taha, G. and Box, G.P. 1999. New method for inferring total ozone and aerosol optical thickness from multispectral extinction measurements using eigenvalue analysis. *Geophys. Res. Lett.*, *26*, 3085-8.
- Thome, K.J., Herman, B.M. and Reagan, J.A. 1992. Determination of perceptible water. *Jnl appl. Met.*, *31*, 157-65.
- Thome, K.J., Smith, M.W., Palmer, J.M. and Reagan, J.A. 1993. Method and instrument for retrieving total columnar water vapor from solar transmittance. In Proceeding of SPIE Int. Soc. Opt. Eng., 1968 *Atmospheric Propagation and Remote Sensing II*, 526-32.
- Twomey, S. 1974. Information content in remote sensing. *Appl. Opt.*, *13*, 942-5.
- Twomey, S. 1977. *Introduction to the mathematics of inversion in remote sensing and indirect measurement*. Elsevier, New York, 243pp.